Enhancement of electrical properties of the thermoelectric compound $Ca_3Co_4O_9$ through use of large-grained powder

Masashi Mikami,[a] Emmanuel Guilmeau, and Ryoji Funahashi
National Institute of Advanced Industrial Science and Technology, Ikeda, Osaka 563-8577, Japan; and Japan Science and Technology Agency, CREST, Kawaguchi, Saitama 332-0012, Japan

Kangji Chong
Osaka Electro-Communication University, Neyagawa, Osaka 572-0833, Japan

Damiel Chateigner
CRISMAT-ENSICAEN Laboratory, UMR CNRS 6508, 14050 Cean Cedex, France

(Received 11 May 2005; accepted 25 May 2005)

Hot-forged $Ca_3Co_4O_9$ (Co349) ceramics were synthesized using large-grained powders prepared by a flux-growth method, and their thermoelectric properties and degree of grain alignment were evaluated. Neutron-diffraction experiments evidenced the effect of grain size on the development of the *c*-axis grain alignment. The optimum grain size was around 7 μm in our hot-forging method. The electrical resistivity (ρ) in the direction parallel to the pressed-plane was more reduced at higher degrees of orientation. Since ρ was reduced without lowering the Seebeck coefficient (*S*), the power factor ($PF = S^2/\rho$) of the Co349 sample was improved and reached 0.8 mW/mK^2 at 1073 K using Co349 grains with average size of around 7 μm. The thermal conductivity (κ) in the direction parallel to the pressed-plane slightly increased with the increase of the grain size, however the improvement of *PF* owing to use of large-grained powder outweighed this negative impact on the κ component of the thermoelectric figure of merit ($Z = S^2/\rho\kappa$).

I. INTRODUCTION

The recent discovery of high thermopower coexisting with low electrical resistivity in layered cobaltites has opened the route to the exploration of thermoelectric materials in oxides.[1–5] Due to their high thermal stability, high tolerance to oxidation, and low toxicity, these oxides are promising candidates for practical use in thermoelectric power generation in air at high temperatures. The conversion efficiency of a thermoelectric material is evaluated by the dimensionless figure-of-merit $ZT = (S^2/\rho\kappa)T$, where *S* is the Seebeck coefficient, ρ is the electrical resistivity, κ is the thermal conductivity, and *T* is the absolute temperature. *ZT* values of single crystals of Na_xCoO_2 and $Ca_3Co_4O_9$ (Co349) along the *ab*-plane exceed 1 at 1000 K,[2,4,5] the estimated criterion for practical application. Due to the layered structure of the Co349 phase, consisting of alternate stacking of a rock-salt-type (Ca_2CoO_3) layer and a CdI_2-type (CoO_2) layer,[6–8] ρ along the *c* axis is considerably higher than that in the *ab*-plane.[6] Given this anisotropy, texturizing the polycrystalline bulk material is indispensable for the achievement of *ZT* high enough for practical application, as it is difficult to grow single crystals large enough for the construction of a thermoelectric device. Some research groups have already reported the fabrication of textured Co349 ceramics by reactive templated grain growth,[9–11] magnetic alignment,[12–14] or utilization of the combined effect of large single crystals and powder.[15] The resulting textured samples show reduced ρ compared to non-aligned sintered-Co349 materials.

To reduce ρ in polycrystalline materials, reduction of the negative influence of grain boundaries on current flow is generally effective. Investigation of the relationship between transport properties and grain size has been reported in Co349 film[16] but not in bulk material. It can, however, be expected that large platelet-shaped grains are easily aligned by uniaxial pressure. In the present study, we prepared textured Co349 bulk materials using large-grained powders. The Co349 grains were grown in the same mixture of K_2CO_3 and KCl as was used as a solvent in a study of crystal growth in the Co349 phase.[17] The thermoelectric properties and the degree of orientation of hot-forged samples were measured to a high degree of precision. The dependence of alignment and thermoelectric properties on grain size in Co349 powder is discussed.

[a]Address all correspondence to this author.
e-mail: m-mikami@aist.go.jp
DOI: 10/1557/JMR.2005.0298

II. EXPERIMENTAL

Co349 powder was prepared by solid-state reaction. A mixture of Co_3O_4 (99.9 %) and $CaCO_3$ (99.5%) at a molar ratio of Ca:Co = 3:4 was ground, calcined at 1073 K for 10 h in air, pulverized, and pressed into pellets, which were sintered at 1153 K for 20 h in an oxygen gas flow and ground into fine powder. To increase the grain size, the prepared Co349 powder was heated at 1123 K for 20 h in a solvent consisting of K_2CO_3 and KCl at a molar ratio of 4:1.[17] The grains were grown at three different weight ratios of solvent to Co349 powder: 10, 20, and 40 wt%. The powder was collected from the solidified materials by dissolving the solvent in distilled water in an ultrasonic washing machine.

The powders were cold-pressed into 30 thin disks, which were finally stacked under uniaxial pressure of 80 MPa into a pellet 6 mm thick and 26 mm in diameter. The layered pellets were then hot-forged at 1153 K for 20 h in air under uniaxial pressure of 5 MPa. The obtained samples, with a diameter of 30 mm and a thickness of 4 mm, were cut into a bar shape with a typical size of $3 \times 3 \times 15$ mm for measurement of thermoelectric properties. In the present paper, the hot-forged samples made of unreacted Co349 powder and the heat-treated Co349 powders with 10, 20, and 40 wt% solvent are expressed as LGCo-0, LGCo-10, LGCo-20, and LGCo-40, respectively.

Crystallographic structure and constituent analyses were performed with powder x-ray diffraction (XRD) using Cu K_α radiation and an energy dispersive x-ray spectrometer (EDX), respectively. The microstructure was observed with a scanning electron microscope (SEM). The grain size of the Co349 powder was measured using a HORIBA particle-size analyzer model LA-500. The degree of grain orientation was evaluated by means of neutron diffraction (D1B line at ILL, Grenoble, France). Neutron diffraction intensities were measured by a curved detector composed of 400 cells spread over 80° (resolution 0.2°) in 2θ. χ scans using an Eulerian cradle were operated from 0° to 90° (step 5°) at a fixed incidence angle θ of 20.6° (Bragg angle of 003 reflection). Since the samples have an axially symmetric (fiber) texture (i.e., random in-plane distribution of crystallite *a* and *b* axes), the complete texture determination can be obtained only by a χ-tilting rotation, the φ being unnecessary. The average volume of our samples was around 500 mm^3, corresponding to a measuring time of around 20 min at each fixed χ step. The orientation distribution (OD) was calculated using the Materials Analysis Using Diffraction (MAUD) package.[18] In this approach, named combined analysis, the Rietveld method[19] for structure determination is combined with the Williams–Imhof–Matthies–Vinel (WIMV) formalism[20] for the calculation of the OD. The texture strength is determined quantitatively in terms of OD density. Using such an approach, a sample without any texture has densities of 1 multiple of a random distribution (mrd) regardless of the (χ, φ) orientation, and a textured sample exhibits minima and maxima of the density values over χ angles.[21] Accurate structural refinement of the Co349 misfit aperiodic phase requires a description in the superspace group formalism for modulated structures. For this reason, we introduced commensurate supercell approximation ($P2_1/m$ space group No. 11) with $b \sim 8b_1 \sim 13b_2$ and a resulting unit cell of $a = 4.8309$ Å, $b = 36.4902$ Å, $c = 10.8353$ Å, and $\beta = 98.1317°$.[7,22] An example of the combined analysis, which illustrates the advantages of this quantitative texture analysis, has already been reported.[23]

The ρ was measured in air in the range of 300–1100 K using a conventional four-probe direct current (dc) technique. *S* was calculated from a plot of thermoelectric voltage against temperature difference using an instrument designed by our laboratory. Two Pt–Pt/Rh (R-type) thermocouples were attached to both ends of the sample using silver paste and the Pt wires of the thermocouples used as voltage terminals. Measured *S* values were corrected by thermopower of the Pt wires to obtain the net *S* values of the samples. κ was evaluated using the Harman method,[24] in which κ was obtained from temperature gradient induced by applied current at room temperature.

III. RESULTS AND DISCUSSION

The microstructure of the prepared powders is shown in Fig. 1. The grain size of Co349 powder appeared to be significantly enhanced by heating in the mixture of K_2CO_3 and KCl. The measurement of average grain size,

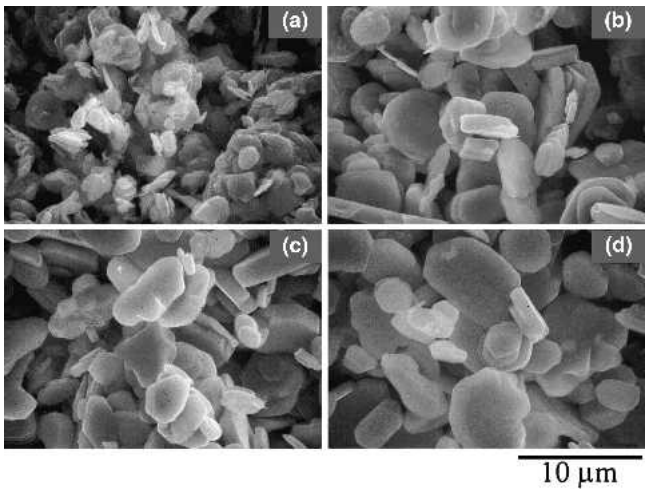

FIG. 1. SEM images of (a) unreacted Co349 powder and powders heat-treated in a solvent mixture of K_2CO_3 and KCl with (b) 10 wt%, (c) 20 wt%, and (d) 40 wt%.

represented in Fig. 2, confirmed this observation. Whereas the untreated powder in the solvent exhibited an average grain size of around 2.4 μm, the addition of 10, 20, and 40 wt% solvent increased grain sizes up to 6.4, 7.1, and 7.9 μm, respectively. This clearly proves the efficiency of solvent addition in improving the grain growth of the Co349 phase. In addition, as shown in Figs. 1(b)–1(d), during the heat treatment in the solvent, the grains grow in the thickness as well as in the length with almost the same average aspect ratio of 5–7. It has moreover been reported that Co349 single crystals millimeters size can be grown in the same solvent by the solution method.[17] The growth of grains with a size of tens or hundreds of micrometers could therefore be achieved by adjusting the amount of solvent and the temperature conditions. The grains have hexagonal shape similar to the single crystal and appear to indicate the high crystallinity. As shown in Fig. 3, XRD patterns of four powders were in agreement with data from the literature on $Ca_3Co_4O_9$ phase.[6] There is no secondary phase. The EDX analysis performed on the powders heated in the solvent showed the grain growth treatment causes no change of the Co349 composition and no incorporation of K^+ or Cl^- ions contained in the solvent. These results indicate that the present grain-growth method has no contamination effects on Co349 powder.

Figure 4 shows SEM images of a fracture transverse section of the hot-forged samples. It can be seen in Figs. 4(b) and 4(c) that LGCo-10 and LGCo-20 are constructed from well-oriented grains with a size of several micrometers. The alignment of the grains is obviously improved when compared to LGCo-0, where small misalignment grains can be observed. On the other hand, the orientation of the grains in LGCo-40 has deteriorated, although the sample consists of larger grains than LGCo-20. The bulk density is also improved by using larger-grained powder, as shown in Table I. Compared to LGCo-20, however, the density of LGCo-40 deteriorates.

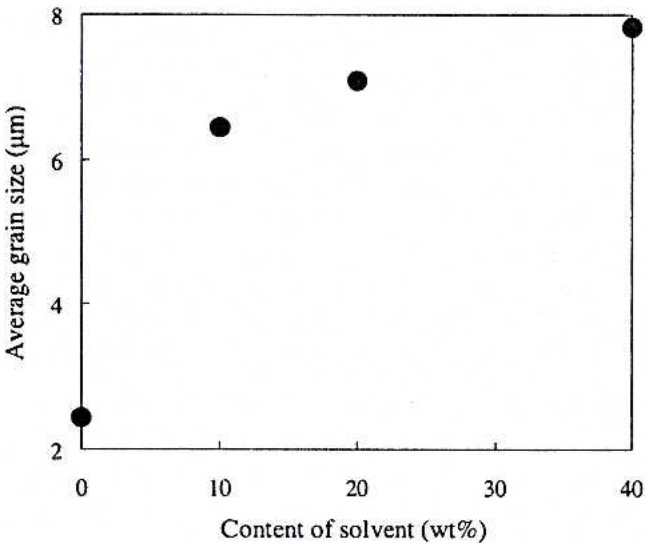

FIG. 2. Relationship between average grain size and weight ratio of solvent.

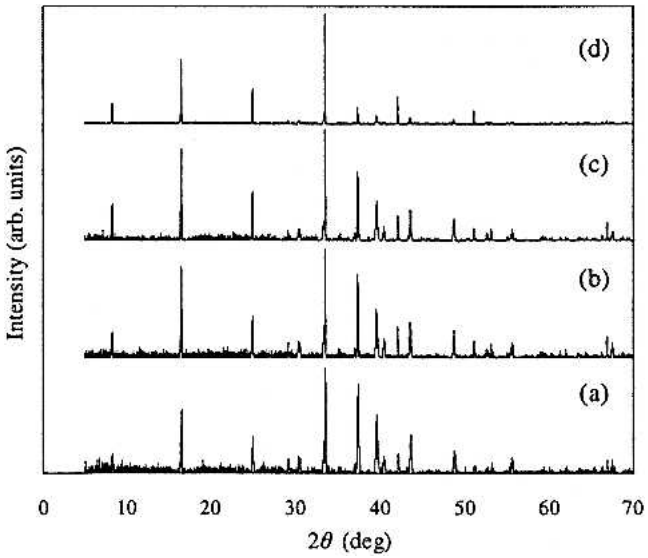

FIG. 3. Powder XRD patterns (Cu K_α radiation) of (a) unreacted Co349 powder and powders heat-treated in a solvent mixture of K_2CO_3 and KCl with (b) 10 wt%, (c) 20 wt%, and (d) 40 wt%.

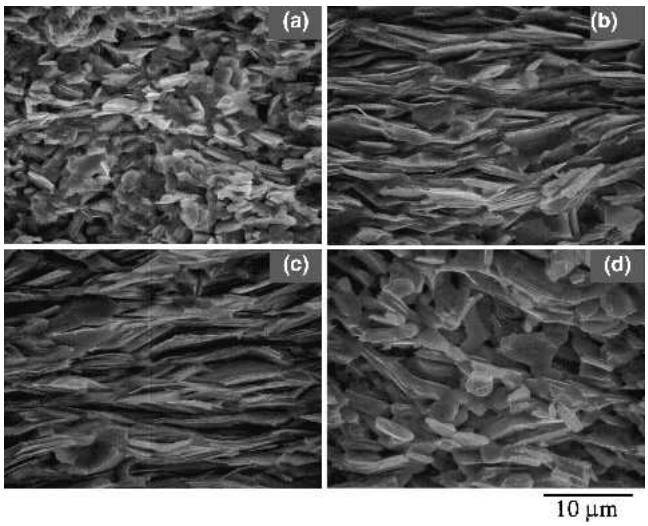

FIG. 4. SEM images of fracture transverse section of (a) LGCo-0, (b) LGCo-10, (c) LGCo-20, and (d) LGCo-40.

TABLE I. Bulk density of hot-forged samples.

LGCo–	Density (g/cm^3)	Relative density (%)[a]
0	4.3	90
10	4.6	96
20	4.6	96
40	4.4	92

[a]The density of $Ca_3Co_4O_9$ single crystal measured by a pycnometer is 4.8 g/cm^3.

We conclude that technical refinements, such as the employment of tape casting using a doctor-blade method, are required to align large grains.

Figure 5 presents the typical neutron-diffraction pattern obtained from the sample LGCo-40 in a 0–90° χ-scan. The inset of Fig. 5 shows schematics of the geometry used for the neutron diffraction (ND) experiment. The 00*l* Bragg intensities from a textured sample decrease with the increase of the χ angle whereas the *hk*0 Bragg intensities grow up. Figure 5 thus highlights without ambiguity the (00*l*) texture of the Co349 phase in the hot-forged sample. In particular, we can clearly observe the disappearance of the 00*l* intensities at $\chi = 90°$ and the enhancement of −201/200 intensities. The behavior of the major peaks shows good compatibility with the theoretical texture and structure; i.e., the χ angle at the maximum of *hkl* Bragg intensity corresponds to the angle between the [001] and the [*hkl*] direction in the monoclinic supercell structure. As an example, 203/−1134 Bragg intensities present a maximum at around $\chi = \overline{60}°$, the value corresponding to the angle between the [203]/[−1134] and [001] directions in the structure.

The question remains of how to estimate from a quantitative point of view the difference in texture strength among the four samples and how to determine any influence of the grain size on the texture development. Due to the complex modulated structure of the Co349 phase, with many peak overlaps in the diffraction pattern, the solution is not easy. To overcome this problem, the combined analysis developed in a previous study on Co349 magnetic alignment material was highly successful in refining the OD and determining with accuracy the fiber texture of the material.[23] We consequently applied the same strategy to our samples (composed of the same crystallographic phase and with almost the same texture). The inverse pole figures for the direction perpendicular to the sample surface are calculated from the OD (Fig. 6). These figures indicate the distribution of [001] direction

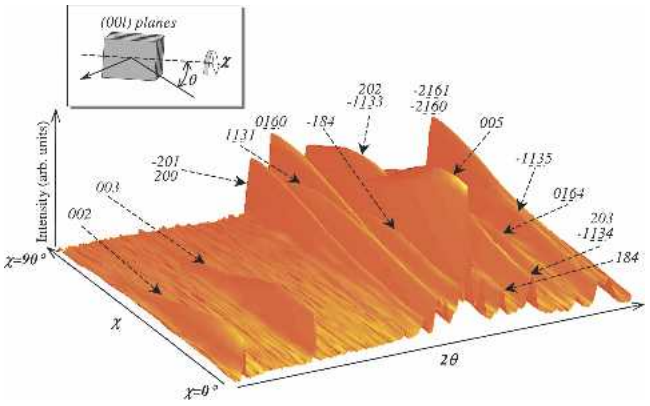

FIG. 5. Neutron diffraction pattern of LGCo-40 sample for a 0° to 90° χ-scan. The inset shows schematics of the geometry used for the ND texture analysis.

of crystallites with the monoclinic system. Two points must be noted: first, we can retrieve here the previously described (001) major component; second, the analysis evidenced quantitatively the effect of grain size on the development of the *c*-axis grain alignment. The samples textured from solvent-grown grains present higher OD maxima, reaching in the LGCo-20 sample a density almost three times higher than that of LGCo-0. This higher distribution density is also correlated to a narrower dispersion of the [00*l*] orientation around the [001] direction. This result provides further evidence of the beneficial effect of larger grain size on texture development. We hypothesize that the decline in the number of grains and the change to a platelike shape enhance the effect of alignment by uniaxial pressure. The elimination of small particles, which disturb the order of the platelets, could be also a factor of promoting the *c*-axis alignment.

The *T*-dependence of ρ along the direction parallel to the pressed plane is shown in Fig. 7. All samples exhibit almost the same *T*-dependence of ρ. A broad maximum around 450 K could correspond to the behavior of ρ in the *ab*-plane of the single crystal Co349.[5] On the other hand, since a steep decrease around 570 K is observed only in polycrystalline hot-forged samples, the rapid reduction could be related to ρ along the *c*-axis or to the electrical properties of the grain boundaries. From the difference in magnitude of ρ, large-grained powder of Co349 can reduce ρ through the *c*-axis grain alignment as mentioned below. One reason for the reduction of ρ is that the increase in the grain size in the hot-forged polycrystalline material, as shown in Fig. 4, simply reduces the number of grain boundaries, at which additional energy is required for carrier traveling. The second is that the improvement of grain alignment reduces the carrier conduction along the *c*-axis, along which ρ is considerably higher than in the *ab*-plane.[6] Moreover, the higher degree of *c*-axis orientation of the grains may decrease the number of boundaries between highly misaligned grains, where the carrier suffers a larger energy loss than at the boundary between well-aligned grains. In other words, the conduction at grain boundaries can be modified by grain alignment. Finally, the increase in bulk density, as listed in Table I, clearly contributes to the reduction of ρ. We conclude that the optimum grain size for the synthesis of highly conductive Co349 bulk material using our procedure is around 7 μm.

As shown in Fig. 8, all samples exhibit almost the same *S*, which was measured along the same direction as ρ. Unlike with ρ, the differences in the microstructure of the polycrystalline materials apparently have little influence on *S* value. The *S* value of the hot-forged samples increases with increase in temperature and reaches 190 μV/K at 1073 K, as with the single-crystal Co349 along the *ab*-plane.[5] Since ρ is reduced without deterioration of *S*, the power factor ($PF = S^2/\rho$) of hot-forged

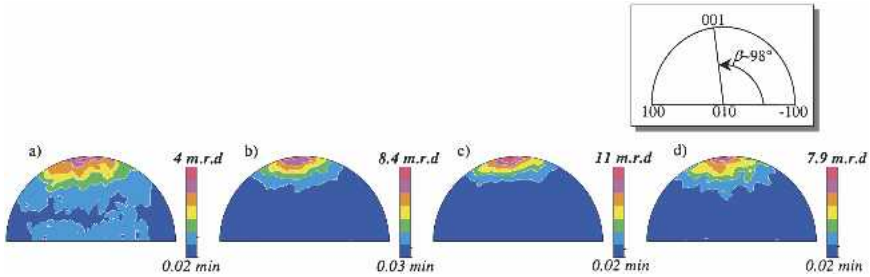

FIG. 6. Inverse pole figures calculated for direction perpendicular to pressed plane (a) LGCo-0, (b) LGCo-10, (c) LGCo-20, and (d) GGCo-40, respectively. Major (001) component is represented in a linear density scale and an equal area projection.

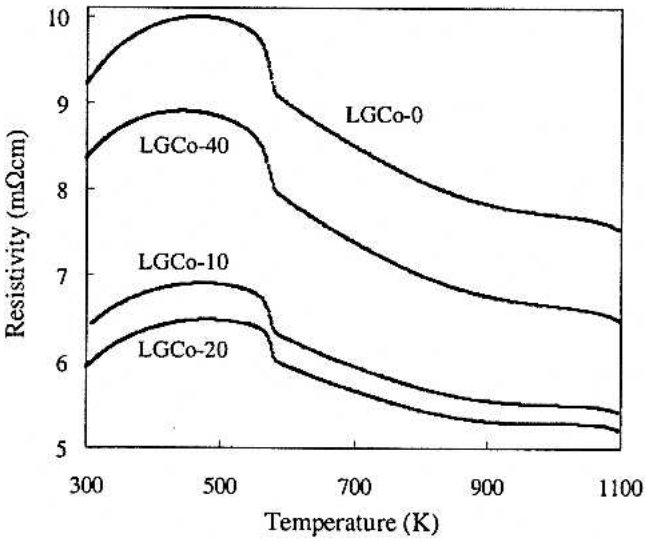

FIG. 7. *T* dependence of ρ measured parallel to pressed-plane.

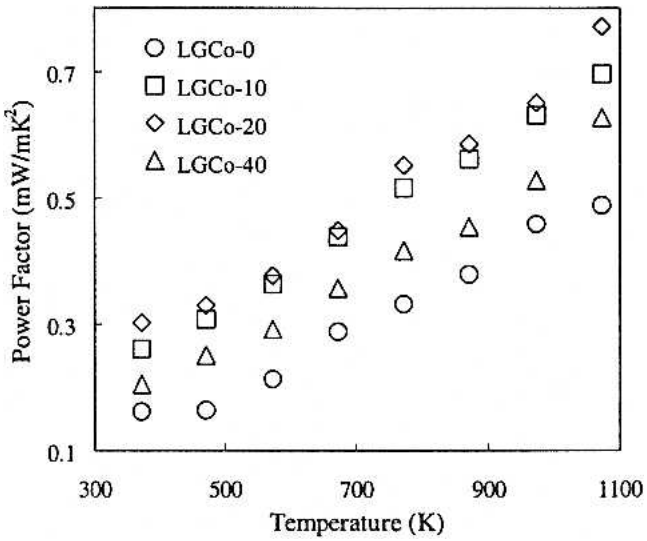

FIG. 9. T-dependence of *PF* for hot-forged samples parallel to pressed-plane.

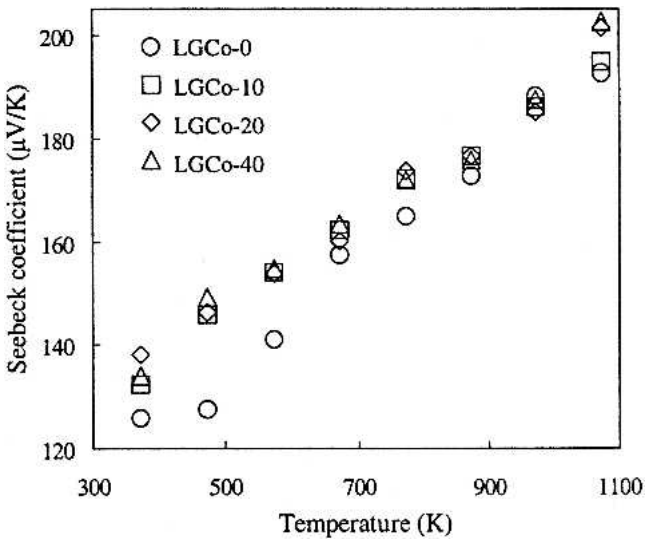

FIG. 8. *S* measured parallel to pressed-plane.

Co349 composed of large-grained powder is improved, as shown in Fig. 9. The *PF* of all samples increased with temperature and that of LGCo-20 reached 0.8 mW/mK^2 at 1073 K. This value is 6–7 times greater than the *PF* reported for non-aligned Co349 ceramics prepared using a conventional solid-state reaction method.[25]

The κ values of LGCo-0 and LGCo-20 in the direction parallel to the pressed-plane were 2.9 and 3.2 W/mK, respectively, at room temperature. The smaller number of grain boundaries caused by the increase of the grain size and the higher degree of grain alignment seem to have little influence on κ value. This result implies that the phonon mean free path (l_{ph}) of Co349 is much smaller than the grain size. The phonon scattering by the modulated structure of Co349[8] and oxygen defects in the Ca_2CoO_3 layer[26] could limit the l_{ph} to a small value. For instance, the reported l_{ph} of the analogous structural layered-cobaltite of $Bi_2Sr_2Co_2O_y$ is 2.8 nm in the *ab*-plane at 300 K,[27] though it is inappropriate to extrapolate the l_{ph} of Co349 from that of $Bi_2Sr_2Co_2O_y$ consisting of heavier ions than Ca and Co in Co349. It has been reported that the ratio of κ in the *ab*-plane to that along the *c*-axis is around 10 in the $Bi_2Sr_2Co_2O_y$ and is much smaller than the anisotropy of ρ around 10^4.[27] Since the distance between CoO_2 layers, which are considered to mainly contribute to the transport of charge carriers, in Co349 structure is shorter than that in $Bi_2Sr_2Co_2O_y$, the

anisotropy of ρ in Co349 is smaller than that in $Bi_2Sr_2Co_2O_y$ and is estimated to be 10^2.[5,6] The reported κ value of the Co349 in the *ab*-plane is about 3 W/mK at room temperature.[5,24] Thus, if the anisotropy of κ in Co349 is as large as that of ρ, κ along the *c*-axis will be 0.03 W/mK, the value of which is less than the theoretical minimum thermal conductivity in solid[28] and is not realistic. Therefore, the anisotropy of κ should be smaller than that of ρ in Co349. In this case, the enhancement of grain alignment can always contribute to the improvement of *Z* because ρ and κ have the same order of contribution in the definition of $Z = S^2/\rho\kappa$. Moreover, since l_{ph} is usually decreased with the increase of temperature, the effect of the grain size on κ will weaken at high temperatures. Thus, the improvement of *PF* of LGCo-20 at 1073 K would not be spoiled by the increase of κ.

IV. CONCLUSIONS

We demonstrated the validity of using large-grained Co349 powder as material for producing thermoelectric Co349 ceramics. The grain size of Co349 powder was successfully enhanced by heat-treatment in an appropriate solvent. Precise texture analysis proved that using large-grained powder could contribute to the enhancement of the degree of orientation. We emphasize that the grain-growth method could be applied to a wide range of materials by using the appropriate solvent and heat-treatment. Thus the beneficial effects on the texturization and the modification of microstructure can be available not only on the Co349 but on other materials which have an anisotropic structure and properties. In the case of Co349, ρ was reduced by improving grain alignment, increasing grain size, and enhancing bulk density. Since ρ was decreased without deterioration of *S*, the *PF* value of the Co349 sample was improved and reached 0.8 mW/mK^2 at 1073 K. This *PF* is the highest value of the Co349 bulk materials to our knowledge. It is expected that the increase of κ caused by the increase of the grain size and the enhancement of the degree of grain alignment is much smaller than the improvement of *PF*. As polycrystalline material generally has lower κ than single crystal, the *ZT* of LGCo-20 at 1073 K may be higher than 0.3, the value of which was calculated using the κ value of the single-crystal Co349 along the *ab*-plane at 1073 K.[5]

ACKNOWLEDGMENT

We wish to thank B. Ouladdiaf from the Institut Laue Langevin (Grenoble, France) for his technical support on the D1B line.

REFERENCES

1. I. Terasaki, Y. Sasago, and K. Uchinokura: Large thermoelectric power in $NaCo_2O_4$ single crystals. *Phys. Rev. B* **56,** 12685 (1997).
2. K. Fujita, T. Mochida, and K. Nakamura: High-temperature thermoelectric properties of $Na_xCoO_{2-\delta}$ single crystals. *Jpn. J. Appl. Phys.* **40,** 4644 (2001).
3. S. Li, R. Funahashi, I. Matsubara, K. Ueno, and H. Yamada: High temperature thermoelectric properties of oxide $Ca_9Co_{12}O_{28}$. *J. Mater. Chem.* **9,** 1659 (1999).
4. R. Funahashi, I. Matsubara, H. Ikuta, T. Takeuchi, U. Mizutani, and S. Sodeoka: An oxide single crystal with high thermoelectric performance in air. *Jpn. J. Appl. Phys.* **39,** L1127 (2000).
5. M. Shikano and R. Funahashi: Electrical and thermal properties of single-crystalline $[Ca_2CoO_3]_{0.7}CoO_2$ with a $Ca_3Co_4O_9$ structure. *Appl. Phys. Lett.* **82,** 1851 (2003).
6. A.C. Masset, C. Michel, A. Maignan, M. Hervieu, O. Toulemonde, F. Studer, and B. Raveau: Misfit-layered cobaltite with an anisotropic giant magnetoresistance: $Ca_3Co_4O_9$. *Phys. Rev. B* **62,** 166 (2000).
7. S. Lambert, H. Leligny, and D. Grebille: Three forms of the misfit layered cobaltite $[Ca_2CoO_3][CoO_2]_{1.62}$—A 4D structural investigation. *J. Solid Chem.* **160,** 322 (2001).
8. Y. Miyazaki, M. Onoda, T. Oku, M. Kikuchi, Y. Ishii, Y. Ono, Y. Morii, and T. Kajitani: Modulated structure of the thermoelectric compound $[Ca_2CoO_3]_{0.62}CoO_2$. *J. Phys. Soc. Jpn.* **71,** 491 (2002).
9. Y. Masuda, D. Nagahama, H. Itahara, T. Tani, W.S. Seo, and K. Koumoto: Thermoelectric performance of Bi- and Na-substituted $Ca_3Co_4O_9$ improved through ceramic texturing. *J. Mater. Chem.* **13,** 1094 (2003).
10. T. Tani, H. Itahara, C. Xia, and J. Sugiyama: Topotactic synthesis of highly-textured thermoelectric cobaltites. *J. Mater. Chem.* **13,** 1865 (2003).
11. H. Itahara, C. Xia, J. Sugiyama, and T. Tani: Fabrication of textured thermoelectric layered cobaltites with various rock salt-type layers by using β–$Co(OH)_2$ platelets as reactive templates. *J. Mater. Chem.* **14,** 61 (2004).
12. M. Sano, S. Horii, I. Matsubara, R. Funahashi, M. Shikano, J. Shimoyama, and K. Kishio: Synthesis and thermoelectric properties of magnetically *c*-axis-oriented $[Ca_2CoO_{3-\delta}]_{0.62}CoO_2$ bulk with various oxygen contents. *Jpn. J. Appl. Phys.* **42,** L198 (2003).
13. Y. Zhou, I. Matsubara, S. Horii, T. Takeuchi, R. Funahashi, M. Shikano, J. Shimoyama, K. Kishio, W. Shin, N. Izu, and N. Murayama: Thermoelectric properties of highly grain-aligned and densified Co-based oxide ceramics. *J. Appl. Phys.* **93,** 2653 (2003).
14. S. Horii, I. Matsubara, M. Sano, K. Fujie, M. Suzuki, R. Funahashi, M. Shikano, W. Shin, N. Murayama, J. Shimoyama, and K. Kishio: Thermoelectric performance of magnetically *c*-axis aligned Ca-based cobaltites. *Jpn. J. Appl. Phys.* **42,** 7018 (2003).
15. R. Funahashi, S. Urata, T. Sano, and M. Kitawaki: Enhancement of thermoelectric figure of merit by incorporation of large single crystals in $Ca_3Co_4O_9$ bulk materials. *J. Mater. Res.* **18,** 1646 (2003).
16. Y. Zhou, I. Matsubara, W. Shin, N. Izu, and N. Murayama: Effect of grain size on electric resistivity and thermopower of $(Ca_{2.6}Bi_{0.4})Co_4O_9$ thin films. *J. Appl. Phys.* **95,** 625 (2004).
17. M. Mikami, S. Ohtsuka, M. Yoshimura, Y. Mori, T. Sasaki, R. Funahashi, and M. Shikano: Effects of KCl addition on the K_2CO_3 flux growth of $Ca_3Co_4O_9$ crystals for a thermoelectric device. *Jpn. J. Appl. Phys.* **42,** 3549 (2003).
18. L. Lutterotti, S. Matthies, and H.R. Wenk: MAUD (Material Analysis Using Diffraction): A user friendly {Java} program for {Rietveld} texture analysis and more, in *Proceedings of the 12th ICOTOM,* Vol. 1, edited by J.A. Szpunar (NRC Research Press, Ottowa, Canada, 1999), p. 1599.
19. H.M. Rietveld: A profile refinement method for nuclear and magnetic structures. *J. Appl. Crystallogr.* **2,** 62 (1969).

20. S. Matthies and G.W. Vinel: On the reproduction of the orientation distribution function of texturized samples from reduced pole figures using the conception of a conditional ghost correction. *Phys. Status Solidi B* **112,** 111 (1982).
21. E. Guilmeau, R. Funahashi, M. Mikami, K. Chong, and D. Chateigner: Thermoelectric properties-texture relationship in highly oriented $Ca_3Co_4O_9$ composites. *Appl. Phys. Lett.* **85,** 1490 (2004).
22. D. Grebille, S. Lambert, F. Bourée, and V. Petricek: Contribution of powder diffraction for structure refinements of aperiodic misfit cobalt oxides. *J. Appl. Crystallogr.* **37,** 823 (2004).
23. E. Guilmeau, D. Chateigner, J. Noudem, R. Funahashi, S. Horii, and B. Ouladdiaf: Rietveld texture analysis of complex oxides: Examples of polyphased Bi2223 superconducting and Co349 thermoelectric textured ceramics characterization using neutron and x-ray diffraction. *J. Appl. Crystallogr.* **38,** 199 (2005).
24. A. Satake, H. Tanaka, T. Ohkawa, T. Fujii, and I. Terasaki: Thermal conductivity of the thermoelectric layered cobalt oxides measured by the Harman method. *J. Appl. Phys.* **96,** 931 (2004).
25. S. Li, R. Funahashi, I. Matsubara, K. Ueno, S. Sodeoka, and H. Yamada: Synthesis and thermoelectric properties of the new oxide materials $Ca_{3-x}Bi_xCo_4O_{9+\delta}$ ($0.0 < x < 0.75$). *Chem. Mater.* **12,** 2424 (2000).
26. J. Shimoyama, S. Horii, K. Otzschi, M. Sano, and K. Kishio: Oxygen nonstoichiometry in layered cobaltite $Ca_3Co_4O_y$. *Jpn. J. Appl. Phys.* **42,** L194 (2003).
27. I. Terasaki, H. Tanaka, A. Satake, S. Okada, and T. Fujii: Out-of-plane thermal conductivity of the layered thermoelectric oxide $Bi_{2-x}Pb_xSr_2Co_2O_y$. *Phys. Rev. B* **70,** 214106 (2004).
28. D.G. Cahill, S.K. Watson, and R.O. Pohl: Lower limit to the thermal conductivity of disordered crystals. *Phys. Rev. B* **46,** 6131 (1992).